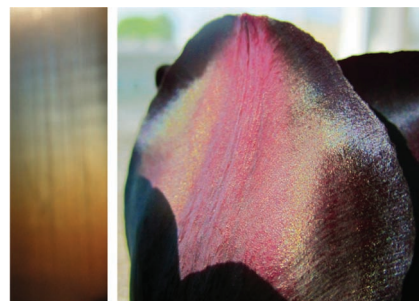


# Structural Color and Iridescence in Transparent Sheared Cellulosic Films

Susete N. Fernandes, Yong Geng, Silvia Vignolini, Beverley J. Glover, Ana C. Trindade, João P. Canejo, Pedro L. Almeida, Pedro Brogueira, Maria H. Godinho\*

Shear transparent cellulose free-standing thin films can develop iridescence similar to that found in petals of the tulip “Queen of the Night.” The iridescence of the film arises from the modulation of the surface into bands periodically spread perpendicular to the shear direction. Small amounts of nanocrystalline cellulose (NCC) rods in the precursor liquid-crystalline solutions do not disturb the optical properties of the solutions but enhance the mechanical characteristics of the films and affects their iridescence. Smaller bands periodicity, not affected by the NCC rods, slightly deviated from the shear direction is also observed. NCCs are crucial to tune and understand the film’s surface features formation. Our findings could lead to new materials for application in soft reflective screens and devices.



## 1. Introduction

In plants, the most common mechanisms by which structures can produce color involve multilayers<sup>[1]</sup> and diffraction gratings.<sup>[2]</sup> This is an inspiration for biomimetic

investigations that aim to obtain materials, which can replicate those structures and form the basis of future optical devices for applications in different fields. Many sophisticated techniques have been developed and also different kinds of materials used to reproduce the iridescence and structural colors found in plants and animals.<sup>[3]</sup> However, a biomimetic route, able to produce those structures using materials found in plants, would shed light on the biological processes at work in growing these structures in nature, and it equips us to fabricate novel photonic structures using low-cost materials in ambient conditions.

Cellulose is found in large quantities in all plants and seems an ideal material with which to mimic their micro- and nanostructures and iridescent colors.

Several years ago, it was discovered that concentrated aqueous solutions of a commercial water-soluble cellulose ether, (hydroxypropyl)cellulose (HPC), displayed iridescent colors that changed with concentration and viewing angle.<sup>[4]</sup> Later it was found that a wide range of cellulose derivatives formed both lyotropic and thermotropic chiral nematic (cholesteric) liquid crystals (LCs). Many attempts had been made to trap the chiral nematic structure in solid films to give colored iridescent films, and in the literature some casting colored films, not sheared, were reported,<sup>[5]</sup>

Dr. S. N. Fernandes, Y. Geng, Dr. A. C. Trindade, Dr. J. P. Canejo, Dr. P. L. Almeida, Prof. M. H. Godinho  
CENIMAT/I3N, Departamento de Ciência dos Materiais,  
Faculdade de Ciências e Tecnologia FCT, Universidade Nova de Lisboa, Campus da Caparica, Caparica, 2829-516, Portugal  
E-mail: mhg@fct.unl.pt

Dr. S. Vignolini  
Cavendish Laboratory, University of Cambridge, JJ Thomson Avenue, Cambridge, CB3 0HE, United Kingdom

Prof. B. J. Glover  
Department of Plant Sciences, University of Cambridge, Downing Street, Cambridge, CB2 3EA, United Kingdom

Dr. P. L. Almeida  
ADF, Instituto Superior de Engenharia de Lisboa ISEL, Instituto Politécnico de Lisboa, R. Conselheiro Emídio Navarro, 1, Lisboa, 1950-062, Portugal

Prof. P. Brogueira  
ICEMS, Department of Physics, Instituto Superior Técnico, Universidade Técnica de Lisboa, Avenida Rovisco Pais, 1, Lisboa, 1049-001, Portugal

In addition, HPC was used as a template and high-surface area porous silica was obtained.<sup>[6]</sup> Sheared casted films were also obtained, studied and used as alignment layers to LCs<sup>[7]</sup> although much less importance was placed on their topological surface structure and eventual application as photonic materials due to a complex network of “band” defects, which are easily identified by polarizing optical microscopy under cross polars.<sup>[8]</sup> Up until now sheared cellulosic films obtained from LC systems are typically described as transparent, and no mention of structural color patterns has been made. Many studies have been performed in order to correlate the appearance of the bands and the rheological behavior of the solutions, but some fundamental questions have not been answered. X-rays results show that the cholesteric order is destroyed in sheared films and that the polymeric molecules undulate along the shear direction.<sup>[9]</sup> Atomic force microscopy (AFM) measurements revealed that the topographical features of the sheared films could be tuned by modifying the films’ processing conditions.<sup>[10]</sup> It was demonstrated that samples prepared from liquid-crystalline solutions showed two periodic structures, a primary and secondary set of bands. The former consists of bands perpendicular to the shear direction while the latter has the bands slightly tilted from that direction. An out-of-plane angle variation of the sinusoidal molecular orientation was also reported.<sup>[10,11]</sup>

In addition to cellulose and the liquid-crystalline phases of cellulose derivatives it was also found that NCC films were capable of reflecting colored light if prepared from liquid-crystalline cellulose suspensions.<sup>[12]</sup> NCC LC templates were used to generate new photonic materials, which can combine mesoporosity with long-range chiral ordering.<sup>[13]</sup> Moreover the incorporation of NCC rods into composite materials with enhanced mechanical properties is not novel and has been investigated systematically in the literature.<sup>[14]</sup> NCC rods seem the perfect material to incorporate in cellulosic water-soluble matrices because of their intrinsic hydrophilic character<sup>[15]</sup> and many studies have described the preparation of films from NCC/polymer mixtures in aqueous media.<sup>[14]</sup>

Recent work shows that certain plant species use micro- and nanostructures to create particular optical effects.<sup>[2,16–18]</sup> The floral iridescence exhibited by *Hibiscus trionum* and *Tulipa kaufmanniana* petals is due to surface diffracting gratings.<sup>[2]</sup> It has also been suggested that structural color generated through diffraction gratings might be widespread among flowering plants.<sup>[1,18]</sup>

In this work, we report for the first time sheared iridescent solid cellulosic films, with tunable mechanical and structural color properties, which mimic the structures found in plants, namely in *Tulipa* petal gratings.

## 2. Experimental Section

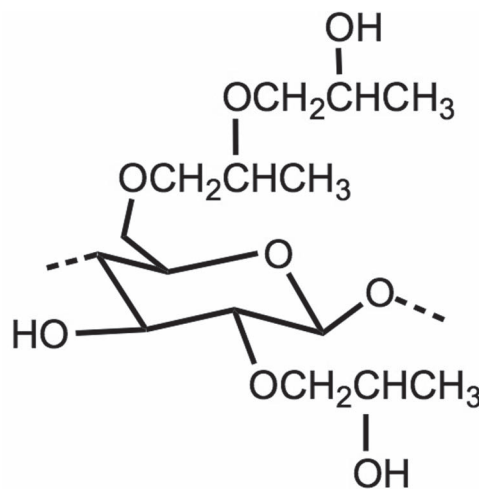
(Hydroxypropyl)cellulose (HPC) was purchased from Sigma–Aldrich ( $\overline{M}_w = 100.000$ ;  $\overline{M}_S = 3.5$ ) and used as received (scheme 1). Nanocrystalline cellulose (NCC) rods were kindly supplied by Professor Doctor D.G. Gray and used without further treatment. 0.1%, 1%, and 5% (w/w calculated taking into account the solid content in solution HPC+NCC) of NCC rods were added to distilled water and the NCC rods dispersed with a UP400S ultrasonic probe from Hielsher (until no NCC clusters could not be detected by eye), these were then used to prepare HPC aqueous solutions. Solutions of HPC in distilled water with concentrations that range from 57 to 65% (w/w) were prepared at room temperature. After the first week, they were stirred every other day and keep away from light for at least 4 weeks until used.

Films were prepared from LC solutions, casted, and sheared simultaneously by moving a calibrated Gardner knife from Braive Instruments at  $1.25 \text{ mm s}^{-1}$ . The films were allowed to dry at room temperature and kept in a controlled relative humidity (20%) chamber until further use. The thickness of the dried films was estimated from the average of 10 measurements by using a Mitutoyo digital micrometer.

The photos of the films were taken with a Casio EX-F1 Exilim Pro photo camera. The bandwidth in polarizing optical microscope (POM) pictures was determined using ImageJ (version 1.45s, <http://imagej.nih.gov/ij/>). Blender, version 2.57b, was used to obtain the 3D draw of the shear-casting knife.

The wavelengths ( $\lambda_0$ ) of the maximum selective reflection peaks were recorded with a Jobin Yvon monochromator H10 Vis mounted on the microscope stage, equipped with a photomultiplier, and a chart recorder. Six measures were obtained for each sample. The film’s textures were observed using a POM Olympus BH2 in transmission and reflection mode coupled to a Canon EOS 550D camera.

SALS measurements were performed by illuminating the films with a laser beam (632 nm) at an incident angle  $\theta_i$  of  $30^\circ$ . The diffraction pattern of each film was projected on a white screen



Scheme 1. Idealized repeating unit of HPC, average degree of substitution  $\overline{DS} = 2$ , average molar substitution  $\overline{MS} = 3$ .

and recorded with a Canon EOS 550D camera. The diffraction was described quantitatively by the grating equation  $N\lambda = \Delta l_1(\sin \theta_d - \sin \theta_i)$  where  $\lambda$  is the wavelength,  $N$  is the diffraction order, and  $\Delta l_1$  is the periodicity of the grating.

The mechanical properties of the samples were registered with a tensile testing machine from Rheometric Scientific (Minimat Firmware Version 3.1). Small rectangular pieces of the cast films, with the dimensions of 5 cm  $\times$  2 cm, were cut in two distinct directions orthogonal to each other (i.e., with the longest dimension of the sample parallel to the direction of the casting shear and perpendicular to it). In addition, the film was stretched uniaxially at a rate of 5 mm min<sup>-1</sup>, along the longest sample dimension. The values of the mechanical properties of a given sample were taken to be the average of the results of six successful measurements.

For the topographical characterization of the films surface, AFM data were acquired using a dimension 3100 spm with a Nanoscope IIIa controller from Digital Instruments (DI). All measurements were performed in tapping mode TM under ambient conditions. A commercial tapping mode etched silicon probe from DI and a 90  $\mu$ m  $\times$  90  $\mu$ m scanner was used.

Scanning electronic microscopy (SEM) was used to imaging the topographical features of the films with a SEM DSM962 model from Zeiss. Gold was deposited on the films by sputtering in an Ar atmosphere, using a 20 mA current, for 30 s at a deposition rate of 3  $\text{Å s}^{-1}$ . Images were captured for an acceleration voltage of 5 kV.

### 3. Results and Discussion

In our work, the material used to prepare replicas of the plant petal surface is a very well-known cellulose derivative, HPC, which can be easily dissolved in water generating liquid-crystalline helicoidal phases with the pitch in the visible range depending on water content.<sup>[4]</sup> We chose this simple water lyotropic system because it is well studied<sup>[4,6–8]</sup> and has appropriate characteristics to incorporate hydrophilic NCC rods. Several lyotropic aqueous solutions ranging from 58% to 65% (w/w) were prepared and in the same range of concentrations 0.1, 1.0, and 5.0% (w/w) of NCC rods was added. All the solutions prepared showed iridescent colors. The maximum peak wavelength ( $\lambda_0$ ) reflected by the samples for incident light normal to the surface may be expressed as,  $\lambda_0 = n_e P \cos \theta$ , where  $n_e$  is the refractive index,  $P$  is the helical pitch, and  $\theta$  is the

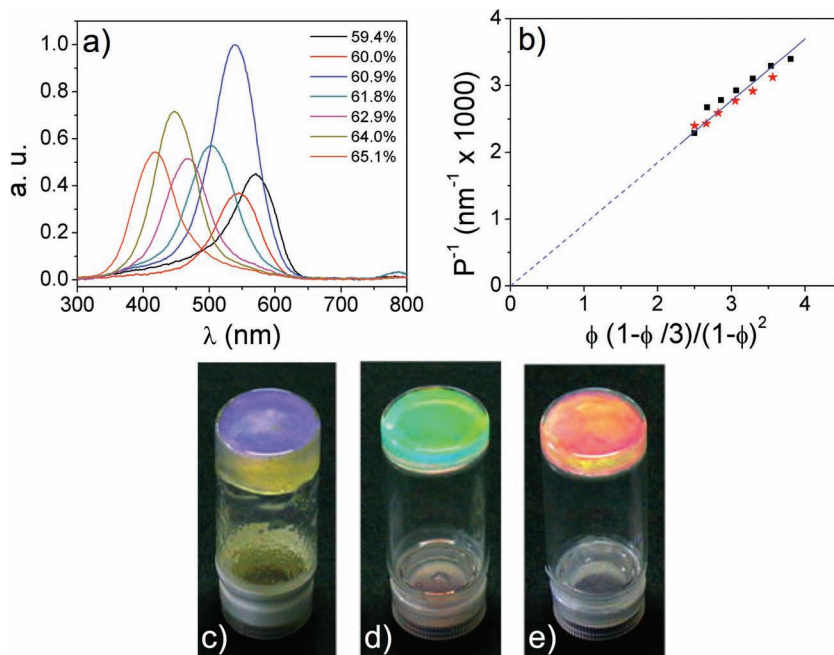


**Figure 1.** Concentrated liquid-crystalline cellulosic solutions; (a) and (b) Visible spectra of anisotropic HPC solutions with nanocrystalline cellulose (NCC) are given along with the reciprocal pitch ( $P$ ) against  $\phi(1 - \phi/3)/(1 - \phi)^2$ , where  $\phi$  is the weight fraction of polymer in (b) HPC/water solutions ( $\blacksquare$ ) and HPC/NCC/water solutions ( $\star$ ). (c) to (e) Liquid-crystalline solutions obtained from HPC/NCC/water solutions, same NCC concentration (0.1%, w/w) with 62%, w/w, 60%, w/w, and 58% w/w of HPC in water, respectively.

angle between the light propagation direction and the helix axis.<sup>[19]</sup> The values of  $\lambda_0$  may therefore be tuned by altering the helical pitch or the average refractive index of the chiral nematic material. We were able to vary  $\lambda_0$  of the solutions in the visible range by increasing the proportion of solvent relative to HPC and NCC rods (Figure 1a and b),  $\lambda_0$  was found to depend on polymer concentration and very slightly on nanowhiskers content. The average refractive indices of the different mixture materials are essentially constant because the two components, crystalline cellulose, and cellulose derivative matrix, have similar refractive indices ( $n_e = 1.54$  and 1.33, respectively). The plot of the reciprocal pitch against  $\phi(1 - \phi/3)/(1 - \phi)^2$  gives a reasonable linear plot, for solutions with and without nanorods, that pass at the origin. Thus, the concentration dependence of the cholesteric pitch is in fairly good agreement with the theory of Kimura et al.<sup>[20]</sup> for different molecular weight samples and different degrees of substituents, per anhydroglucose unit. The increase of the pitch with water content was reported long ago for the HPC/water system.<sup>[21,22]</sup> The solvent was found to stabilize the cholesteric liquid-crystalline phase above a certain critical concentration.<sup>[21]</sup> The liquid-crystalline phase arrangement can be attributed to the relatively stiff cellulose backbone. In fact, the persistence length of HPC in aqueous solution varies from 13 to

21 nm,<sup>[23]</sup> which makes HPC a semirigid polymer forcing a parallel orientation of the chains. The chirality of the cellulose chain imparts a twist to the parallel arrangement, and the flexible side chains and the solvent allow the polymer molecules to migrate and form an equilibrium helical configuration. The fact that the helical pitch varies slightly by adding 0.1% (w/w) NCC rods is an indication that the liquid crystalline characteristics of these solutions is not much affected by the presence of the NCC rods (Figure 1c to e). NCC rods, with a diameter of 5 to 70 nm and a length of 100 to 250 nm<sup>[14]</sup> seem to pack along the oriented liquid-crystalline segments with the rods' main axis parallel to the cellulosic backbone, which forms the polymeric matrix. In order to incorporate the NCC rods into the anisotropic HPC matrix first they were dispersed in water, which was possible due to the NCC rods' hydrophilic nature. The liquid-crystalline solutions were then prepared using the water NCC doped system (Figure 1c to e).

Solid films were fabricated by spreading the anisotropic solutions, with the help of a calibrated shear-casting knife, at room temperature, in an appropriate Teflon mold, schematically shown in Figure 2a. This procedure allows the precise control of the shear casting flow speed ( $v$ ) (1 mm s<sup>-1</sup>) and enables the ready removal of the films without damaging them. After solvent-controlled evaporation, the solid cast shear films had an average thickness between 14 and 30  $\mu\text{m}$ . Due to the large surface area, good dispersibility, low susceptibility to bulk moisture absorption and high elastic modulus (138 GPa<sup>[14]</sup>) NCC rods have been incorporated into composite materials, enhancing their mechanical properties.<sup>[24]</sup> In this work, we used NCC filler as a probe, which can influence the mechanical properties of the films but does not destroy the liquid crystalline characteristics of

the composite material. In fact, adding 0.1% of NCC rods implies that the Young's modulus of the films, as well as the tensile strength, measured in perpendicular (*Per*) and parallel (*Par*) directions to the casting, increased by a factor of 2.5 and 3.2 for *Par* and 3.0 and 2.2 for *Per*, respectively, compared with films prepared from HPC anisotropic solutions, as can be seen in Figure 2c. Because of the high degree of molecular orientation, the HPC and the HPC/NCC films exhibit high modulus and strength along the shear direction and the mechanical strength in the transverse direction is low (Figure 2c). These anisotropic mechanical properties are consistent with the molecular orientation, which results from the flow of the liquid-crystalline solution under shear stress. The fact that the Young's modulus and strength is much higher for HPC/NCC compared with HPC films, along the shear direction, is an indication that NCC rods align along this direction when the films are prepared. NCC rods enhanced the brittle behavior along this direction as well as in the *Per* direction and act as a stiffener to the anisotropic cellulose matrix, which is also reflected in the strength deformation values for *Par* and *Per* directions (Figure 2c). The significant improvement in the matrix modulus was also observed for other NCC composite materials, namely poly(styrene-co-n-butyl acrylate) (PBA) latex/NCC, and the enhanced mechanical properties have been attributed to a hydrogen bond network,<sup>[24]</sup> which can not be ruled out in our system. NCC rods and HPC have available hydroxyl groups, which could generate a hydrogen-bond network between the filler and the cellulose-based matrix. The most important fact is that a very small amount of NCC rods added to the liquid-crystalline solutions implies a large improvement in the mechanical properties of the anisotropic films and did not disrupt the liquid crystalline order of the solutions.

In order to investigate the textures of the free-standing HPC and HPC/NCC films, we analyzed them by POM and a similar banded structure was observed (Figure 3a). This band structure consists of bright bands and dark lines alternate and perpendicular to the shear when viewed between cross polarizers, the textures observed are not compatible with a cholesteric lamellar structure. These patterns are usually described as a relaxation process, which occur immediately after the end of a shear applied to polymer liquid-crystalline solutions.<sup>[25]</sup> They are described in detail in the literature and are always obtained after shearing cellulosic liquid-crystalline solutions.<sup>[26]</sup> Band structures were associated with a long-range undulation of

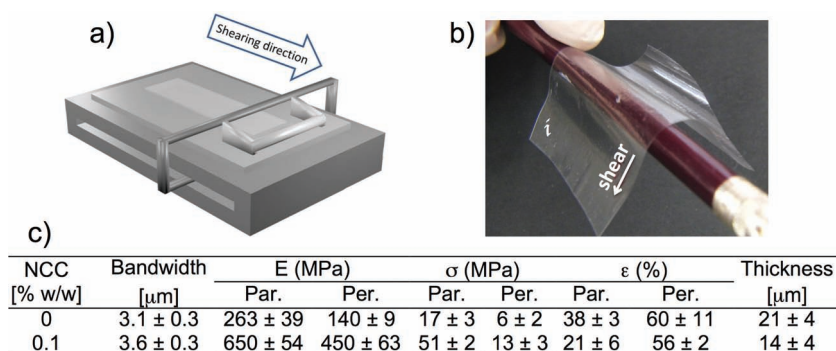


**Figure 2.** A shear-casting knife was used to produce the films, as shown schematically in (a). A free-standing sheared film prepared from HPC/NCC water 60% (w/w) solution is shown in (b i), the white arrow represents the shear direction. Table (c) shows the bands perpendicular to the shear direction width, Young's modulus (E), the tensile stress ( $\sigma$ ), strain deformation ( $\epsilon$ ), and the thickness of the films prepared from an HPC and HPC/NCC 62% (w/w) water liquid-crystalline solution. *Par* and *Per* means that the mechanical stress strain measurements were performed along the parallel and the transverse directions to the shear casting direction, respectively.

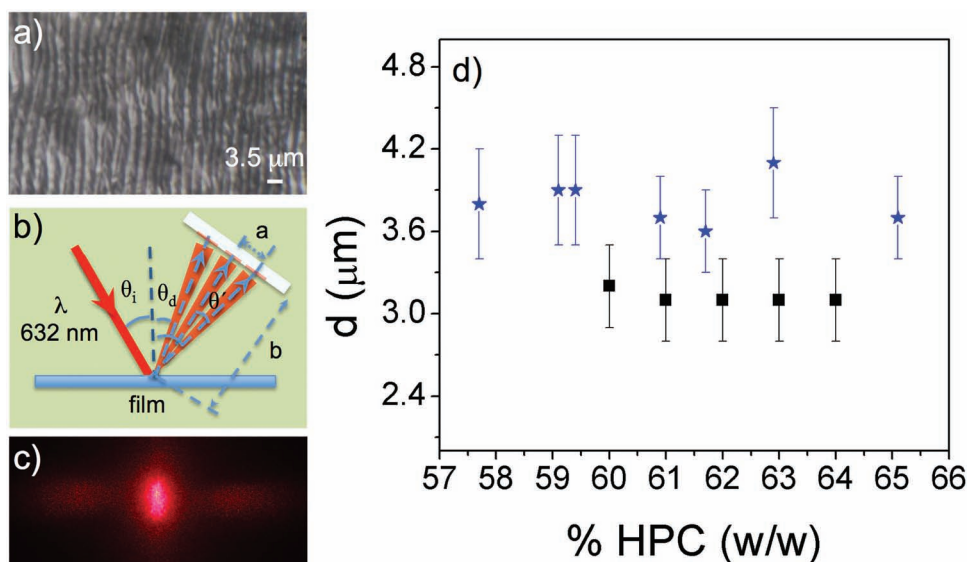


**Figure 3.** Characterization of large grating periodicities running perpendicular to shear direction detected by POM and SALS; (a) transmission polarizing optical microscopy image, taken between cross polarizers, shows bands, which occur after the end of shear applied to the preparation and locked in the films after solvent evaporation. (b) Schematic representation of the SALS measurement geometry and detector set-up. The laser light ( $\lambda = 632$  nm) incidence angle is,  $\theta_i$ , equal to  $30^\circ$ . The light is reflected by the surface of the films at an angle  $\theta_d = \theta_i \pm \theta'$ . (c) Diffraction pattern of one of the gratings ( $4.0 \pm 2$   $\mu\text{m}$ ) in reflection pattern observed for a solid film cast from a cellulosic solution with NCC (0.1%, w/w). (d) Influence of solution concentration and NCC particles on large gratings periodicity -  $d$  - for shear casted solid films prepared from different HPC/water by weight concentration (%HPC (w/w)), (★) films with HPC/NCC and (■) HPC films.

the director orientation<sup>[27]</sup> and can be frozen in the solid films after solvent evaporation.<sup>[28]</sup>

The air surface structure of the free-standing films was also investigated by small-angle light scattering (SALS) (see schematic in Figure 3b). The diffraction pattern, caused by the interaction of the LASER ( $\lambda = 632$  nm) light with the transparent and uniform material, showed a periodicity  $d$  along the direction perpendicular to shear. This indicates that the material surface develops a periodical grating perpendicular to shear direction. In average, the surface periodicities of the HPC and HPC+NCC films are of the order of  $3.1 \pm 0.3$  and  $3.8 \pm 0.4$   $\mu\text{m}$ , respectively, and are not much affected by polymer content. Increasing the material strength and endurance, due to the presence of the NCC rods, could lead to more pronounced effects in bands spacing if the periodic oscillation of the orientation of the director is only attributed to contraction strains of the sheared sample induced by stress relaxation after cessation of flow. Nevertheless, the periodicity for HPC/NCC films is slightly higher, which is a consequence of the anisotropic properties of the films and the brittle behavior promoted by adding the NCC rods.

To further investigate the bands structure, the HPC/NCC films surfaces were investigated by AFM (Figure 4) and two different scale periodical gratings were observed: the primary set of bands, already characterized by SALS, perpendicular to the shear direction, and a smoother texture characterized by a secondary periodic structure containing

“small” bands. The analysis of the height profile at the two cross sections, AA' and BB', is shown in Figure 4b. Cross section AA' was taken along the shear direction. The periodicity of the larger bands,  $\Delta\ell_1$ , and the average peak-to-valley height for these bands,  $h_1$ , were determined from AA' height profile plot, as indicated. Cross section BB' was taken along the direction of the secondary periodic “small” bands. The periodicity of the “small” bands,  $\Delta\ell_2$ , and their peak-to-valley height,  $h_2$ , were measured from the BB' height profile plot, as indicated in Figure 4a and b. The arrows on the top of the image along the AA' and BB' lines mark the points used for the measurements performed in the height profile plots. In accordance with the SALS results, for the primary set of bands, the parameters  $\Delta\ell_1$  and  $h_1$  are higher for films prepared with NCC rods and do not depend strongly on polymer content (Figure 3d and 4d). Unlike primary bands the secondary bands  $\Delta\ell_2$  and  $h_2$  values, for all the HPC and HPC/NCC cellulosic films prepared and reported in the literature,<sup>[10]</sup> show a net tendency to decrease with polymer content. Figure 4c shows a top view image of the height scan of the surface shown in Figure 4a. The out-of-plane angle of the sinusoidal variation in the molecular orientation,  $\theta_p = \tan^{-1} \left( \frac{h_1}{\Delta\ell_{OP}} \right)$ , is obtained from the projection of the peak of one secondary band on the horizontal plane ( $\Delta\ell_{OP}$ ).

NCC rods play a key role because their presence does not affect in the same way the mechanical properties of the films and the periodicities of the primary and second

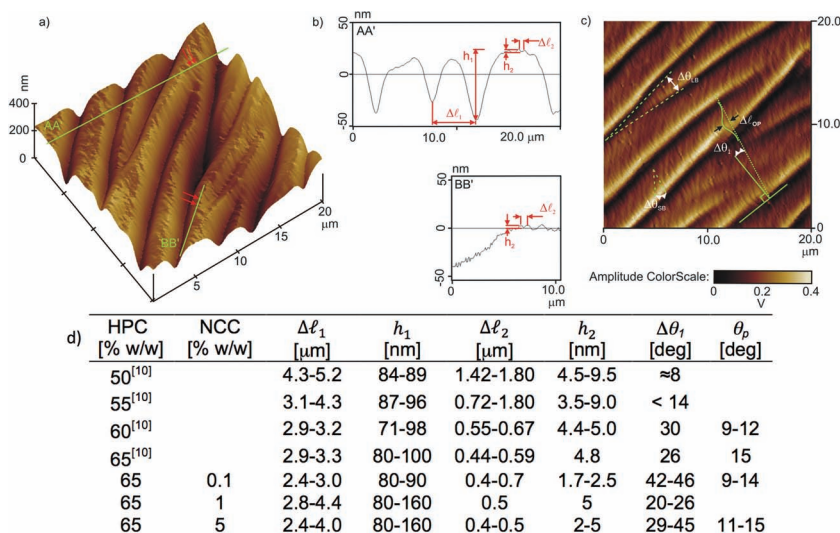


**Figure 4.** AFM images. (a) 3D topography image ( $20 \times 20 \mu\text{m}^2$  scan) of the free surface of a sheared film prepared from 60% HPC+0.1% NCC (w/w) solution at a shear rate  $v = 1.25 \text{ mm s}^{-1}$ . (b) Height profile analysis at the two cross sections: AA' and BB'. The arrows on the top of a view image along AA' and BB' lines mark the points used for the measurements of the height profile. AA' highlights characteristic properties of the primary bands ( $h_1$  and  $\Delta l_1$ ) and BB' those of the secondary bands ( $h_2$  and  $\Delta l_2$ ). (c) Top view image of the amplitude scan of the surface shown in (a). The secondary set of bands is at angle  $\Delta \theta_1$  to the shear direction. The horizontal distance between the line that joins both valley coordinates of a secondary band and the point obtained from the projection of the peak of the same secondary band on the horizontal plane,  $\Delta l_{op}$  is used to calculate the out-of-plane angle of the sinusoidal variation in the molecular orientation,  $\theta_p$ . Defects occurring in the film surface give branched extra layers inserted at an angle  $\Delta \theta_{LB}$ .  $\Delta \theta_{SB}$  is the angle that the small bands make with the shear direction.

sets of bands. These facts seem to be an indication that the development and periodicities of the bands are mainly ruled by the cholesteric liquid crystal characteristics imposed by the initial precursor solutions. The pitch of the cholesteric solution and the related values of the anisotropic elastic constants of the material can therefore be mainly responsible for the variation in size of the secondary bands, observed experimentally.

#### 4. Summary

The results obtained indicate that the optical and mechanical properties of the HPC and HPC/NCC films can be tuned as a function of the initial characteristics of the liquid-crystalline solutions and quantity of NCC rods.

In fact NCC rods are very interesting materials that can originate chiral nematic organization and like other cholesteric materials, which can be duplicated in polymer networks,<sup>[29]</sup> they can be replicated in pure silica films.<sup>[13]</sup> Stacked layers that result from the helical pitch of the chiral nematic phase were obtained. Such periodic structures, with a repeating distance of the order of  $P/2$ , can also be found in thin sections of biological materials. A

twisted plywood model was proposed by Bouligand<sup>[30]</sup> to account for such architecture.

In the case of our sheared films, X-rays<sup>[27]</sup> and POM (Figure 3a) measurements indicate that the cholesteric organization of the initial solution is destroyed and that a bundle of warped helicoidal fiber-like structures developed with the fibers residually oriented along the shear direction. The sheared banded cellulosic films are typically described as transparent with no mention of structural or iridescent colors (see photo Figure 2b). We found that these transparent films have the potential to generate shifting patterns of color as the viewer moves, they possess the ability of reflect one particular peak wavelength of light at one angle, and another peak wavelength at a second angle. This iridescence covers some different colors in the region of the visible spectrum (Figure 5a–d). We also found that if the bottom surface of the free-standing films is observed under a microscope, in the reflection mode, different interference colors can be seen at the border of some line defects (Figure 5e). Iridescence and the

majority of structural color can be produced by coherent light scattering, which occurs when the distribution of light-scattering elements, and the resulting phase relationship of reflected light waves, is precisely ordered. The simplest type of coherent light scattering is that of thin film interference, which gives color to soap bubbles and oil-slicked puddles. Diffraction gratings consisting of a reflective surface over which runs a series of ordered and precisely spaced parallel grooves, and can also produce iridescence.<sup>[31]</sup> The colors observed for the cellulosic films described in this work can be attributed to the 3D periodic bands surface gratings observed by AFM (Figure 4a) at the micro and nano scale. Nevertheless, SEM pictures taken perpendicular to the film surface show a layered structure connected by a network of “holes” (Figure 5h and g). The border of the cross section layers is adorned with “pins,” which seems reminiscent of a structure that exists in the layers. The bottom film surface was observed by SEM and is essentially flat. By POM in the reflection mode, black lines can be observed and must correspond to the border of the layers observed by SEM in the film cross section. The spacing between the layers observed by SEM is of the order of microns and at small confined regions on the film surface some interference colors can be observed

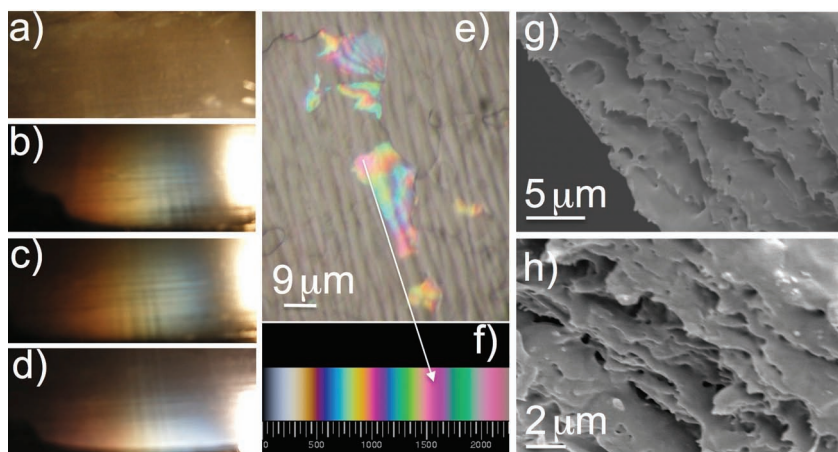


**Figure 5.** (a) to (d) correspond to reflection photos taken at different incident angles of white light films illumination. The variation of the film colors depends on the light incidence angle and for normal incidence the films look macroscopically transparent (a). (b) to (d) shifting patterns of color as the view angle changes. The different colors when viewed from different angles, iridescence, are due to the periodic structure of the material. (e) POM photo in reflection mode, parallel polars, showing some interference colors at the border of black line defects. These colors are an indication that at small regions the distance between the layers, that can be observed in the film cross-section by SEM, are of the order of 120 to 250 nm calculated by taking into account the color transition blue-magenta as observed and in the Newton scale (f) and the refractive index of HPC (1.33). (g) and (h) represent SEM pictures of the cross section of the sheared HPC films. A layered structure parallel to the films surface can be observed and also a periodic reminiscent “pins” from a structure, which exists in between the layers. The periodic structure that exists in between the layers seems responsible for the angle color dependence of the films.

(Figure 5e). The sequence of colors in those minor domains of the films is similar to the Newton series reflected from a thin film of oil on water.<sup>[31]</sup> The Newton series is a very characteristic sequence of repeated color bands grouped into orders. Taking into account, the refraction index of the films (1.33) and the Newton series, displayed in Figure 5f, the thickness between those layers, restricted to small

sample domains, varies from 1.5 to 2  $\mu\text{m}$ , which for normal incidence is out of the visible range.

The surface characteristic patterns found by AFM, as well as the lamellar structure observed by SEM in our cellulosic films, can also be seen in plants.<sup>[31]</sup> In fact we observed the surface of Tulip “Queen of the Night” petals (Figure 6a). The SEM image in Figure 6b shows the periodical striation, of about 1.5  $\mu\text{m}$  spaced, responsible of the iridescence of the petal. The single epidermal layer, once is peeled from the petal, is transparent and the contribution from the ordered grating can be separated from the underneath layer contacting pigment and the iridescence can be measure using a K-space imaging system (Bertrand Lens), (Figure 6d).

## 5. Conclusion

In this work, we found that the mechanical and optical properties of micrometer thin transparent cellulosic films can be tuned by modifying precursor liquid crystalline characteristics of the system

and by adding cellulose nano rods.

We report for the first time that those banded films can show iridescence, which is very similar to those found in Tulip “Queen of the Night” petals.

This simple and low-cost cellulosic material seems ideal to mimic the structures that can be found in plants, namely the type of gratings observed in the petals of many plant species.

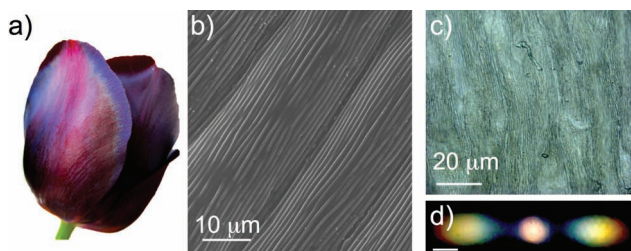


**Figure 6.** Tulip Queen of the Night petals gratings (a) Picture of the Tulip Queen of the Night flower. (b) The SEM image shows the striated epidermis of the flower; the periodicity is in the order of 2  $\mu\text{m}$  comparable to the one of the films. (c) Optical microscope reflection image of the peeled epidermal layer of the petal. The transparent epidermal layer maintains the regularity of the striation also after the peeling process. (d) K-space imaging of the peeled epidermal layer showing iridescence. Please note that the scale bar in (d) correspond to 20°.

**Acknowledgements:** This research was supported by the Portuguese Science and Technology Foundation (FCT) through contracts PTDC/CTM/099595/2008/2009, PTDC/CTM/101776/2008, PTDC/FIS/110132/2009, and PEst-C/CTM/LA0025/2011 (Strategic Project - LA 25 - 2011-2012). S.N.F., Y.G., and A.C.T. acknowledge FCT for grants SFRH/BPD/78430/2011, SFRH/BD/63574/2009 and SFRH/BDP/65133/2009, respectively. We thank Professor D.G. Gray and Dr. E. Kloser for the kindly supply of nanocrystalline cellulose rods and E. Moyroud and U. Steiner for useful discussion.

Received: June 22, 2012; Revised: September 7, 2012; Published online: November 21, 2012; DOI: 10.1002/macp.201200351

**Keywords:** cellulose free-standing films; iridescence; liquid-crystalline polymer solutions; nanocrystalline cellulose rods; structural colors

- [1] C. Hébant, D. W. Lee, *Am. J. Botany* **1984**, *71*, 216.
- [2] H. M. Whitney, M. Kolle, P. Andrew, L. Chittka, U. Steiner, B. J. Glover, *Science* **2009**, *323*, 130.
- [3] M. Kolle, P. M. Salgard-Cunha, M. R. J. Scherer, F. M. Huang, P. Vukusic, S. Mahajan, J. J. Baumberg, U. Steiner, *Nat. Nanotechnol.* **2010**, *5*, 511.
- [4] R. S. Werbowyj, D. G. Gray, *Mol. Cryst. Liq. Cryst.* **1976**, *34*, 97.
- [5] V. Arrighi, J. M. G. Cowie, P. Vaqueiro, K. A. Prior, *Macromolecules* **2002**, *35*, 7354.
- [6] A. Thomas, M. Antonietti, *Adv. Functional Mater.* **2003**, *13*, 763.
- [7] N. Mori, M. Morimoto, K. Nakamura, *Macromolecules* **1999**, *32*, 1488.
- [8] N. Mori, M. Morimoto, K. Nakamura, *Adv. Mater.* **1999**, *11*, 1049.
- [9] C. Sena, M. H. Godinho, C. L. P. Oliveira, A. M. F. Neto, *Cellulose* **2011**, *18*, 1151.
- [10] M. H. Godinho, J. G. Fonseca, A. C. Ribeiro, L. V. Melo, P. Brogueira, *Macromolecules* **2002**, *35*, 5932.
- [11] S. S. Patnaik, T. J. Bunning, W. W. Adams, J. Wang, M. M. Labes, *Macromolecules* **1995**, *28*, 393.
- [12] X. M. Dong, T. Kimura, J. F. Revol, D. G. Gray, *Langmuir* **1996**, *12*, 2076.
- [13] K. E. Shopsowitz, H. Qi, W. Y. Hamad, M. J. MacLachlan, *Nature* **2010**, *468*, 422.
- [14] D. Klemm, K. Friederike, S. Moritz, T. Lindstrom, M. Ankerfors, D. Gray, A. Dorris, *Angew. Chem. Int. Ed.* **2011**, *50*, 5438.
- [15] X. Cao, H. Dong, C. M. Li, *Biomacromolecules* **2007**, *8*, 899.
- [16] B. J. Glover, H. M. Whitney, *Ann Botany* **2010**, *105*, 505.
- [17] S. Vignolini, M. M. Thomas, M. Kolle, T. Wenzel, A. Rowland, P. J. Rudall, J. J. Baumberg, B. J. Glover, U. Steiner, *J. R. Soc. Int* **2012**, *9*, 1295.
- [18] M. Kolle, in *Photonic Structures Inspired by Nature*, Ph.D Thesis, University of Cambridge, UK, Springer-Verlag, Berlin **2011**, p. 40.
- [19] H. L. De Vries, *Acta Crystallogr.* **1951**, *4*, 219.
- [20] H. Kimura, M. Hosino, H. Nakano, *J. Phys. Soc. Jpn.* **1982**, *51*, 1584.
- [21] R. S. Werbowyj, D. G. Gray, *Macromolecules* **1984**, *17*, 1512.
- [22] Y. Onogi, J. L. White, J. F. Fellers, *J. Polym. Sci., Polym. Phys. Ed.* **1980**, *18*, 663.
- [23] R. S. Werbowyj, D. G. Gray, *Macromolecules* **1980**, *13*, 69.
- [24] V. Favier, G. R. Canova, J. Y. Cavaille, H. Chanzy, A. Dufresne, C. Gauthier, *Polym. Adv. Technol.* **1995**, *6*, 351.
- [25] G. Kiss, R. S. Porter, *Mol. Cryst. Liq. Cryst.* **1980**, *60*, 267.
- [26] B. Ernst, P. Navard, *Macromolecules* **1989**, *22*, 1419.
- [27] M. H. Godinho, D. Filip, I. Costa, A.-L. Carvalho, J. L. Figueirinhas, E. M. Terentjev, *Cellulose* **2009**, *16*, 199.
- [28] J. Wang, M. M. Labes, *Macromolecules* **1992**, *25*, 5790.
- [29] M. Mitov, N. Dessaud, *Nature Materials* **2006**, *5*, 361.
- [30] Y. Bouligand, *Solid State Phys.* **1978**, *14*, 259.
- [31] D. Reis, B. Vian, J.-C. Roland, *Micron* **1994**, *25*, 171.